atmosphere

MDPI

Article

Application and Improvement of the Particle Swarm Optimization Algorithm in Source-Term Estimations for Hazardous Release

Jinshu Lu †, Mengqing Huang †, Wenfeng Wu *, Yonghui Wei and Chong Liu

Department of Naval Architecture and Maritime, Zhejiang Ocean University, Zhoushan 316022, China; ljs_ljs@zjou.edu.cn (J.L.); huangmengqing@zjou.edu.cn (M.H.); z20086100067@zjou.edu.cn (Y.W.); liuchong@zjou.edu.cn (C.L.)

* Correspondence: wuwf@zjou.edu.cn

† These authors contributed equally to this work.

Abstract: Hazardous gas release can pose severe hazards to the ecological environment and public safety. The source-term estimation of hazardous gas leakage serves a crucial role in emergency response and safety management practices. Nevertheless, the precision of a forward diffusion model and atmospheric diffusion conditions have a significant impact on the performance of the method for estimating source terms. This work proposes the particle swarm optimization (PSO) algorithm coupled with the Gaussian dispersion model for estimating leakage source parameters. The method is validated using experimental cases of the prairie grass field dispersion experiment with various atmospheric stability classes. The results prove the effectiveness of this method. The effects of atmospheric diffusion conditions on estimation outcomes are also investigated. The estimated effect in extreme atmospheric diffusion conditions is not as good as in other diffusion conditions. Accordingly, the Gaussian dispersion model is improved by adding linear and polynomial correction coefficients to it for its inapplicability under extreme diffusion conditions. Finally, the PSO method coupled with improved models is adapted for the source-term parameter estimation. The findings demonstrate that the estimation performance of the PSO method coupled with improved models is significantly improved. It was also found that estimated performances of source parameters of two correction models were significantly distinct under various atmospheric stability classes. There is no single optimal model; however, the model can be selected according to practical diffusion conditions to enhance the estimated precision of source-term parameters.

Keywords: source-term parameter estimation; forward dispersion model; particle swarm optimization algorithm; gas release; atmospheric diffusion conditions

check for updates

Citation: Lu, J.; Huang, M.; Wu, W.; Wei, Y.; Liu, C. Application and Improvement of the Particle Swarm Optimization Algorithm in Source-Term Estimations for Hazardous Release. *Atmosphere* **2023**, *14*, 1168. https://doi.org/10.3390/atmos14071168

Academic Editor: Martin Piringer

Received: 2 May 2023
Revised: 15 July 2023
Accepted: 17 July 2023
Published: 19 July 2023

Copyright: © 2023 by the authors. Licensee MDPI, Basel, Switzerland. This article is an open access article distributed under the terms and conditions of the Creative Commons Attribution (CC BY) license (https://creativecommons.org/licenses/by/4.0/).

1. Introduction

The release and diffusion of hazardous gas during production, transportation, and storage can pose a serious threat to public safety and the natural environment. The rapid and accurate identification of leakage source information is crucial for the rational disposal of hazardous gas leakage and diffusion accidents. Source information is an essential prerequisite for determining safety separation and emergency evacuation areas and forecasting the development of hazardous substances, which contributes to formulate scientific emergency-response strategies. However, source information is often not readily available, and when it is not directly available, source-term estimation becomes the primary means of obtaining source information. Source-term estimation utilizes observed concentrations of gas dispersion and meteorological information as well as other a priori information to determine source parameters, such as the strength and location of the source [1]. Consequently, conducting research on source-term estimation is crucial for public safety, economic development, and the natural environment.

A significant area of studies at present is enhancing the accuracy of source-term estimations [2]. The precision of the forward dispersion model and the method employed to detect source information are critical elements influencing the accuracy of source-term estimations [3]. Most previous studies on source-term estimations have concentrated on the application of various methods [2,4–7]. To date, the methods for source-term estimation can be broadly divided into indirect and direct methods. Direct methods, which typically require an extensive placement of sensors in a vast region of the monitoring area and have the disadvantage of higher costs, use the anomaly information identified by the monitoring network to determine the source information. Hence, indirect methods based on probabilistic statistical theory approaches [8–10] and optimization methods [11–15] are commonly used. The posterior probability distribution of the estimated results can be obtained using prior information in the methods based on the probability statistical theory, and then the uncertainty of the estimation results can be obtained by the random sampling of the posterior probability distribution [1,7]. However, for methods based on the probabilistic statistical theory, the sampling procedure is extremely time-consuming; thus, the computational efficiency of the algorithm needs to be enhanced to handle the identification of source-term information during emergencies. Conversely, optimization methods are deemed to be more appropriate to an actual accident application with regard to computational speed [6], which is utilized to identify estimation outcomes of source terms that cause the error (defined by means of an objective function) between simulated concentration values of the forward diffusion model and observed concentration values minimal, thus transforming source-term estimations into optimization problems of fitting concentration fields [12]. Various optimization methods, such as the pattern search (PS) [11] algorithm and simplex algorithm (NM) [6,11], have been employed in succession to estimate the source terms. However, when the initial values are not chosen properly, such algorithms tend to collapse into local minima, which cannot ensure convergence to the global optimal solution. Heuristic optimization algorithms, including genetic algorithms (GAs) [2,3,6,11,16], simulated annealing algorithms (SAs) [11,14], evolutionary strategies (ESs) [15], particle swarm optimization (PSO) [5,6,17,18], and chicken swarm optimization (CSO) [5], are widely utilized since they have no dependency on initial value selection and can obtain the global optimal solution. To evaluate effective methods for source-term estimations, Ma et al. [11] compared the performances of GA, PS, SA, and NM algorithms and their coupled algorithms. The test results showed that the performance of different algorithms for estimating different source parameters varied more significantly, with the difference in the relative error being around 12% for source strength and around 25.1% for source location. Mao et al. [5] investigated the performance of various bionic optimization methods (BIOs) for source parameter estimations and found that the bacterial foraging optimization approach (BFO) had the best estimation accuracy for the source parameters. These studies demonstrate that the selection of algorithms affects the performance in estimating the source parameters. The PSO algorithm, which has the advantages of rapid convergence, a simple structure, and few parameters to adjust, is applied to solve high-dimensional nonlinear problems and has been commonly employed for detecting source parameters [5,18,19]. Qiu et al. [20] estimated the source parameters utilizing the PSO algorithm based on expectation maximization (EM). Both Chen [6] and Ma [18] found that the PSO algorithm performed better for source-term estimations than other algorithms (e.g., GA, NM, ant colony optimization (ACO), and firefly algorithm (FA)) and was a useful tool for estimating source parameters. Consequently, this paper utilizes the PSO algorithm to estimate the source parameters. Additionally, the precision of the forward diffusion model in the source estimation process has significant effects on the estimation accuracy of the source term [1,21].

For satisfying the computational efficiency requirements of the source-term estimation method, researchers typically select the computationally efficient Gaussian model [6,9,12] as the forward dispersion model, which results in the low accuracy of the source-term estimation due to Gaussian model defects. For this problem, the artificial neural network (ANN) was introduced into the field for gas dispersion modeling [11,20]. However, the prediction outcomes of artificial neural networks beyond the training range are insuffi-

ciently accurate. Due to the limitation of the precision of artificial neural network, it is hard to acquire accurate source-term estimation outcomes. Mao et al. [22] discovered that the dispersion parameters in the Gaussian dispersion model were crucial to the accuracy of the source-term estimation because they affected the precision of the dispersion model. Moreover, Mao et al. [3] optimized the Gaussian dispersion model's dispersion parameters to enhance the accuracy of the source-term estimation. This presents a novel idea for enhancing the accuracy of source-term estimations.

Initially, this paper combines the PSO algorithm with Gaussian model for estimating leakage source parameters, given the effect of atmospheric dispersion conditions on the performance of the method for source-term estimations [23]. The proposed approach is tested utilizing experimental cases from the prairie grass field dispersion experiment [24], which includes diverse diffusion conditions, and the effect of atmospheric diffusion conditions on estimation outcomes is investigated. Nevertheless, due to the inapplicability of Gaussian dispersion models under extreme atmospheric stability, more accurate dispersion models have not been established under extreme atmospheric conditions, resulting in some discrepancy in the source-term estimates from the actual values. Accordingly, this paper presents improved models, namely, the Gaussian model with linear correction coefficients and Gaussian model with polynomial correction coefficients under various diffusion conditions, to enhance the precision of estimated outcomes of the PSO algorithm.

2. Methodology

2.1. Forward Dispersion Model Selection

Forward dispersion models are the primary factor affecting the precision of estimated outcomes of source parameters, and many dispersion models have been applied to source-term estimations, including the Gaussian model [3,6,11], computational fluid dynamics (CDF) model [25], and Lagrangian stochastic (LS) model [26]. Among these dispersion models, the CDF and LS models are inappropriate to rapidly estimate the leakage of source information due to their excessive computational cost. In contrast, the Gaussian model is frequently applied to source-term estimations due to rapid computation and highly accurate predictions. This paper selected the Gaussian plume model to simulate concentration distributions, with the wind direction along the x-axis and crosswind direction along the y-axis. The concentration (g/m^3) simulated by the Gaussian plume model at the (x, y, z) location is shown in Equation (1):

$$C(x,y,z) = \frac{Q_0}{2\pi u \sigma_y \sigma_z} \exp\left(-\frac{1}{2} \times \frac{(y-y_0)^2}{\sigma_y^2}\right) \times \left\{\exp\left(-\frac{1}{2} \times \frac{(z-z_0)^2}{\sigma_z^2}\right) + \exp\left(-\frac{1}{2} \times \frac{(z+z_0)^2}{\sigma_z^2}\right)\right\} \quad (1)$$

u (m/s) is the mean wind velocity; Q_0 (g/s) is the source release strength; x_0 (m) is the horizontal coordinate of the leakage source; y_0 (m) is the vertical coordinate of the leak source; and z_0 (m) is the vertical distance of the leakage source from the ground. The lateral dispersion parameter σ_y (m) and the vertical dispersion parameter σ_z (m) are associated with the atmospheric diffusion conditions and the distance between the horizontal scale of the sampling point location and the horizontal scale of the leakage source [24]. Atmospheric stability was classified using the Pasquill classification method [27].

2.2. Object Function

The idea of source-term estimation is to utilize optimization methods to locate the source information that minimizes the error (defined by the means of an objective function) between simulated concentration values of the forward diffusion model and observed concentration values by sensors. Source-term estimations are transformed into optimization problems of fitting concentration. That is, the objective function is optimally solved. The objective function of the optimization problem is formulated, as illustrated in Equation (2), for estimating the source parameters:

$$\text{Objective function}: f(Q_0, x_0, y_0, z_0) = \min \sum_{i=1}^{n} [C_{mon,i} - C_{cal,i}(Q, x, y, z)]^2 \quad (2)$$

where $C_{mon,i}$ (g/m^3) and $C_{cal,i}$ (g/m^3) are, respectively, the actual observed and simulated concentration at the ith monitoring point; n denotes the number of sensors; Q_0 (g/s) is the source release strength; x_0 (m) is the horizontal coordinate of the leakage source; y_0 (m) is the vertical coordinate of the leak source; and z_0 (m) is the vertical distance of the leakage source from the ground.

2.3. PSO Algorithm

The PSO algorithm [17] was developed to be inspired by the predatory behavior of birds. Each particle searches at a certain speed through the search space and aggregates towards the prior individual's optimal position and population's optimal position to search for optimal solutions in complex spaces.

The computational process can be described as follows: firstly, the particle swarm is randomly initialized, namely, the positions and velocities of the particles are randomly initialized, and the fitness value of each particle is calculated; then, the optimization was sought by iteration. In each iteration, each particle updates its position and velocity by tracking the individual and the population optimal solutions until the termination condition is reached. The velocities and positions of the particles are updated according to Equations (3) and (4):

$$v_{iD}(n+1) = w.v_{iD}(n) + c_1 r_1(p_{iD} - x_{iD}(n)) + c_2 r_2(p_{gD} - x_{iD}(n)) \quad (3)$$

$$x_{iD}(n+1) = x_{iD}(n) + v_{iD}(n+1) \quad (4)$$

where w is the inertia weight, c_1 and c_2 are learning factors, and r_1 and r_2 are random numbers. x_{iD} and v_{iD} are the position and velocity of particle i in D-dimensional space, respectively. p_{iD} and p_{gD} are the prior individual optimal position and population optimal position, respectively. The computational procedure of the PSO algorithm is shown in Figure 1.

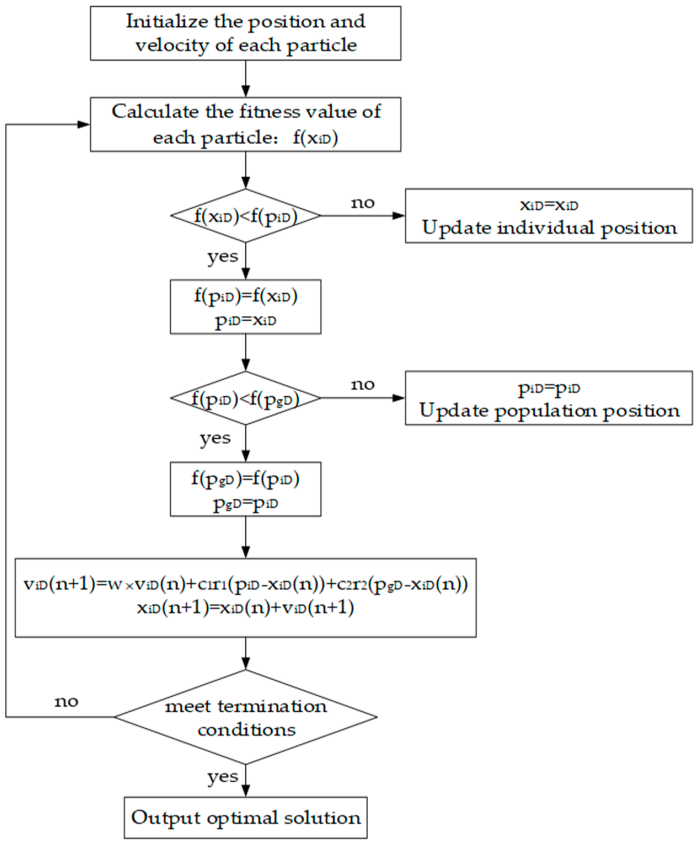

Figure 1. Framework of the PSO algorithm.

2.4. Definition of Score Index

Due to the numerous parameters to be estimated, the comprehensive score index is constructed to assess the estimated precision of the source parameters. The comprehensive score index consists of a series of sub-score indexes, each of which represents the estimated precision of different parameters. Referring to the study by [6], the sub-score indexes were designed as follows:

$$S_Q = |(Q_r - Q_e)/\,Q_r| \tag{5}$$

$$S_x = \frac{|x_e - x_r\,|}{\max\{|x_{\max} - x_r|, |x_r - x_{\min}|\}} \tag{6}$$

$$S_y = \frac{|y_e - y_r\,|}{\max\{|y_{\max} - y_r|, |y_r - y_{\min}|\}} \tag{7}$$

$$S_z = \frac{|z_e - z_r\,|}{\max\{|z_{\max} - z_r|, |z_r - z_{\min}|\}} \tag{8}$$

where the subscripts "r" and "e", respectively, represent the real values and the estimates. The subscripts "min" and "max" denote the lower and upper bounds of the searching scope of every parameter in the algorithm. S_Q represents the estimated precision of the leakage source strength. S_x, S_y, S_z describe the estimated precision of the leakage source location by estimation error and searching scope. If x_e, y_e, z_e reach the boundary of the searching scope, then the correspondent score is set to 1. When there is a score over 1, set it to 1. Thus, the range for each score index is [0,1]. Based on the abovementioned sub-score indexes, the comprehensive score index for the estimated effect of the source term can be obtained as follows:

$$S = \left(w_1 S_Q + w_2 S_x + w_3 S_y + w_4 S_z\right)/4 \tag{9}$$

where, w_i, $i = 1, 2, 3, 4$ represent the weight of each sub-score index, which can be flexibly adjusted to highlight certain parameters according to the experimental results and analytical requirements. This paper assigned equal weight to each sub-score index.

3. Results and Discussion

The effectiveness of the PSO algorithm for source-term estimations is validated utilizing the prairie grass experiment [24], which contains 68 consecutive releases of SO_2 gas. In each experiment, the SO_2 gas was released from the source at 0.46 or 1.5 m (the last four tests) for approximately 10 min. As shown in Figure 2, the mean concentrations were observed by sensors disposed on five semicircular arcs of 50, 100, 200, 400, and 800 m from the leakage source. The experiment was implemented under various atmospheric diffusion conditions. Each test was classified using Pasquill atmospheric stability classes [27], which can be classified as stability classes A to F. This paper selected six trials under various diffusion conditions to prove the estimation performance of the PSO algorithm, and the detailed experimental information is presented in Table 1. Figure 3a–f shows the comparison between observed and simulated concentrations by the Gaussian model utilizing experimental parameters for six selected trials under atmospheric stability classes A to F. Sensors were disposed of on five semicircular concentric arcs, which were represented with alternating gray and white backgrounds, and the sensors were disposed counterclockwise on each semicircular arc.

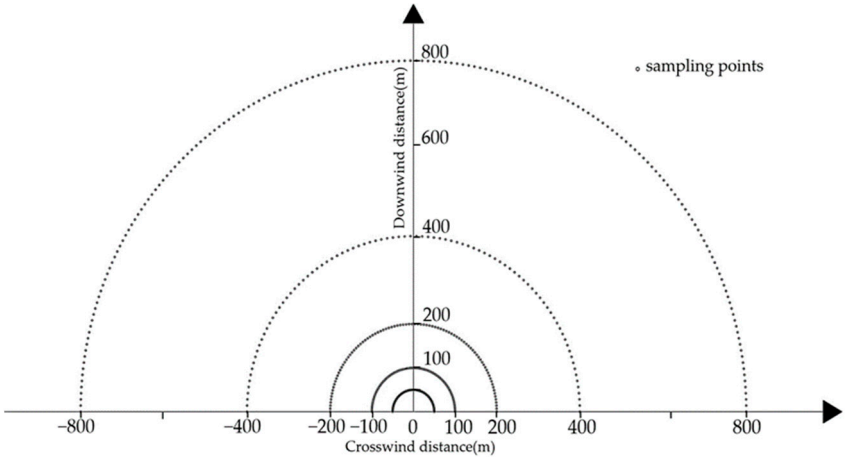

Figure 2. Arrangement of the sensors.

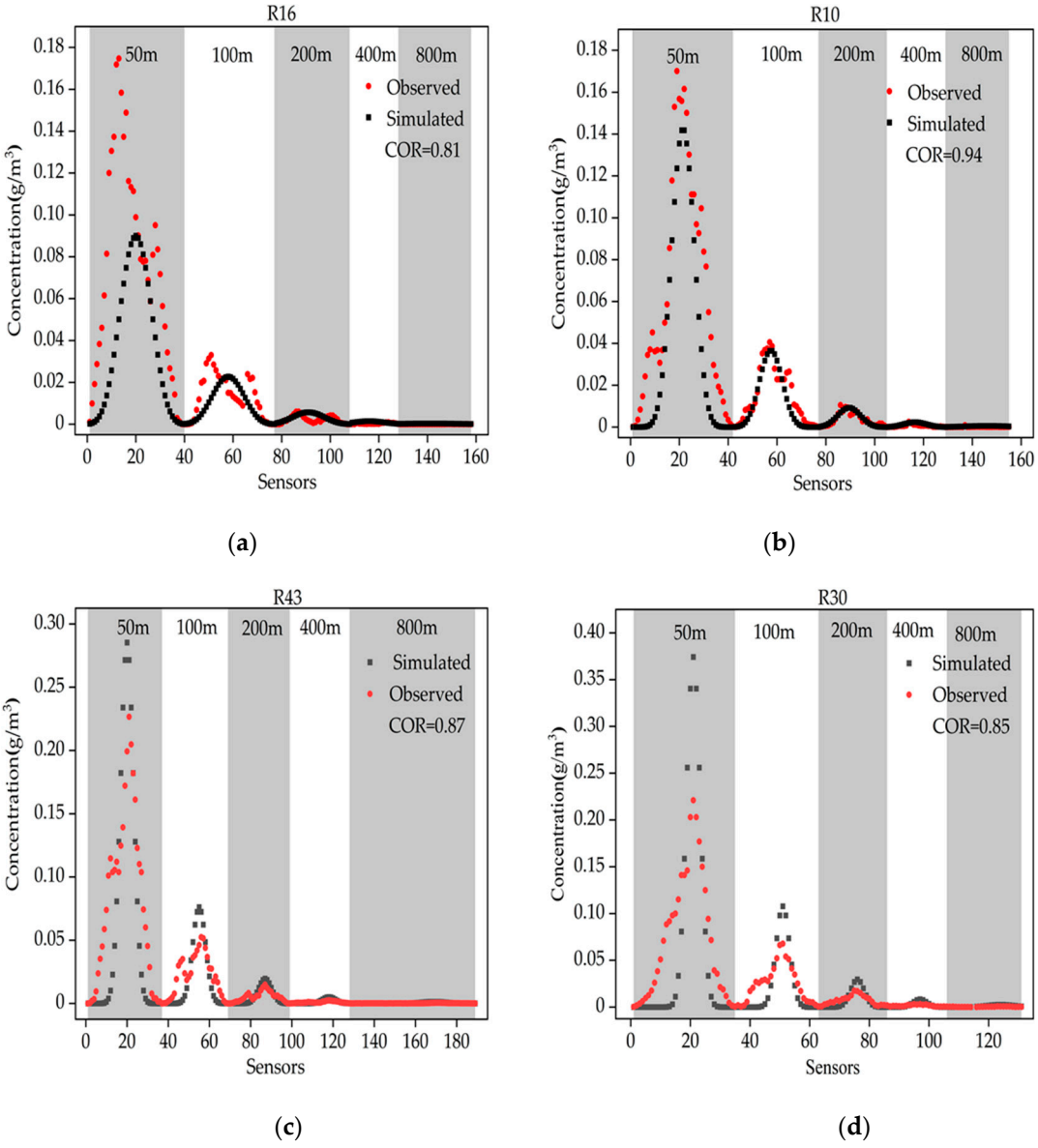

Figure 3. *Cont.*

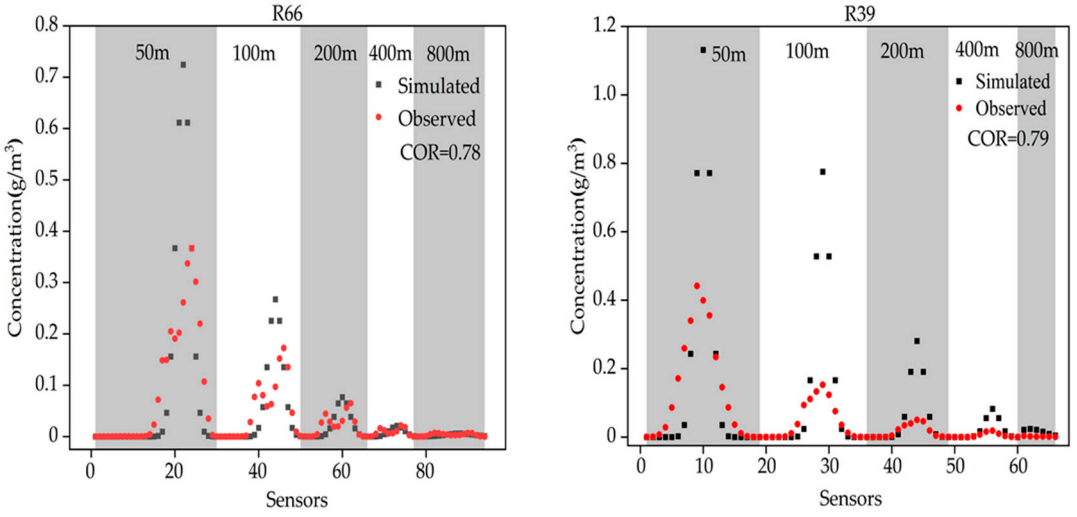

(**e**) (**f**)

Figure 3. Comparison of observed and simulated concentrations by the Gaussian model utilizing experimental parameters: (**a**) R16 with stability class A; (**b**) R10 with stability class B; (**c**) R43 with stability class C; (**d**) R30 with stability class D; (**e**) R66 with stability class E; (**f**) R39 with stability class F. Sensors are disposed of in five semicircular concentric arcs, which are represented with alternating gray and white backgrounds, and the sensors are disposed counterclockwise on each semicircular arc.

Table 1. Conditions of the experimental implementation and diffusion parameters.

Case	(Q_0, x_0, y_0, z_0)	U (m/s)	Atmospheric Stability Class	σ_y(m)	σ_z(m)
R16	(93.0, 0, 0, 0.46)	2.96	A	$\sigma_y = 0.22\Delta x/(1+0.0001\Delta x)^{0.5}$	$\sigma_z = 0.20\Delta x$
R10	(92.1, 0, 0, 0.46)	4.15	B	$\sigma_y = 0.16\Delta x/(1+0.0001\Delta x)^{0.5}$	$\sigma_z = 0.12\Delta x$
R43	(98.9, 0, 0, 0.46)	4.68	C	$\sigma_y = 0.11\Delta x/(1+0.0001\Delta x)^{0.5}$	$\sigma_z = 0.08\Delta x/(1+0.0002\Delta x)^{0.5}$
R30	(98.4, 0, 0, 0.46)	6.28	D	$\sigma_y = 0.08\Delta x/(1+0.0001\Delta x)^{0.5}$	$\sigma_z = 0.06\Delta x/(1+0.0015\Delta x)^{0.5}$
R66	(43.1, 0, 0, 1.50)	2.56	E	$\sigma_y = 0.06\Delta x/(1+0.0001\Delta x)^{0.5}$	$\sigma_z = 0.03\Delta x/(1+0.0003\Delta x)$
R39	(40.7, 0, 0, 0.46)	3.12	F	$\sigma_y = 0.04\Delta x/(1+0.0001\Delta x)^{0.5}$	$\sigma_z = 0.016\Delta x/(1+0.0003\Delta x)$

Note: $\Delta x = x - x_0$, which is the difference between the horizontal scale of the sampling point location and the horizontal scale of the leakage source.

3.1. Estimated Results of Six Selected Trials

The estimated results of the source parameters [Q_0, x_0, y_0, z_0] of six selected trials under different atmospheric stability classes are demonstrated in Figure 4. The estimated results were based on 10 independent runs of PSO, where the means values were marked with gray bars and the 95% confidence intervals were marked with red error bars. Satisfactory results were attained (Figure 4a) regarding the estimation of the source strength. With the exception of tests R66 (stability class E) and R39 (stability class F), the estimated values of source strength Q_0 for other trials were quite close to the actual values, with a source strength score index less than 0.1. This demonstrates that the PSO algorithm can estimate source strength accurately and with a reasonable estimation accuracy. However, the location parameter x_0 had the poorer performance (Figure 4b). Only R10 could estimate x_0 quite accurately and its confidence interval contained the actual value x_0; the estimated values of x_0 for the remaining trials departed from the actual values to some extent. Especially, compared to the remaining trials, R66 and R39 overestimated x_0, whose scoring index S_x was greater than 0.1. The location parameters y_0 and z_0 had outstanding estimation performances (Figure 4c,d); the score indexes of y_0 and z_0 were less than 0.02 and 0.05, respectively, in all tests. The comprehensive score index for all trials was less than or equal to 0.03. As a conclusion, the results demonstrate that it is feasible to utilize the PSO algorithm for source-term estimations.

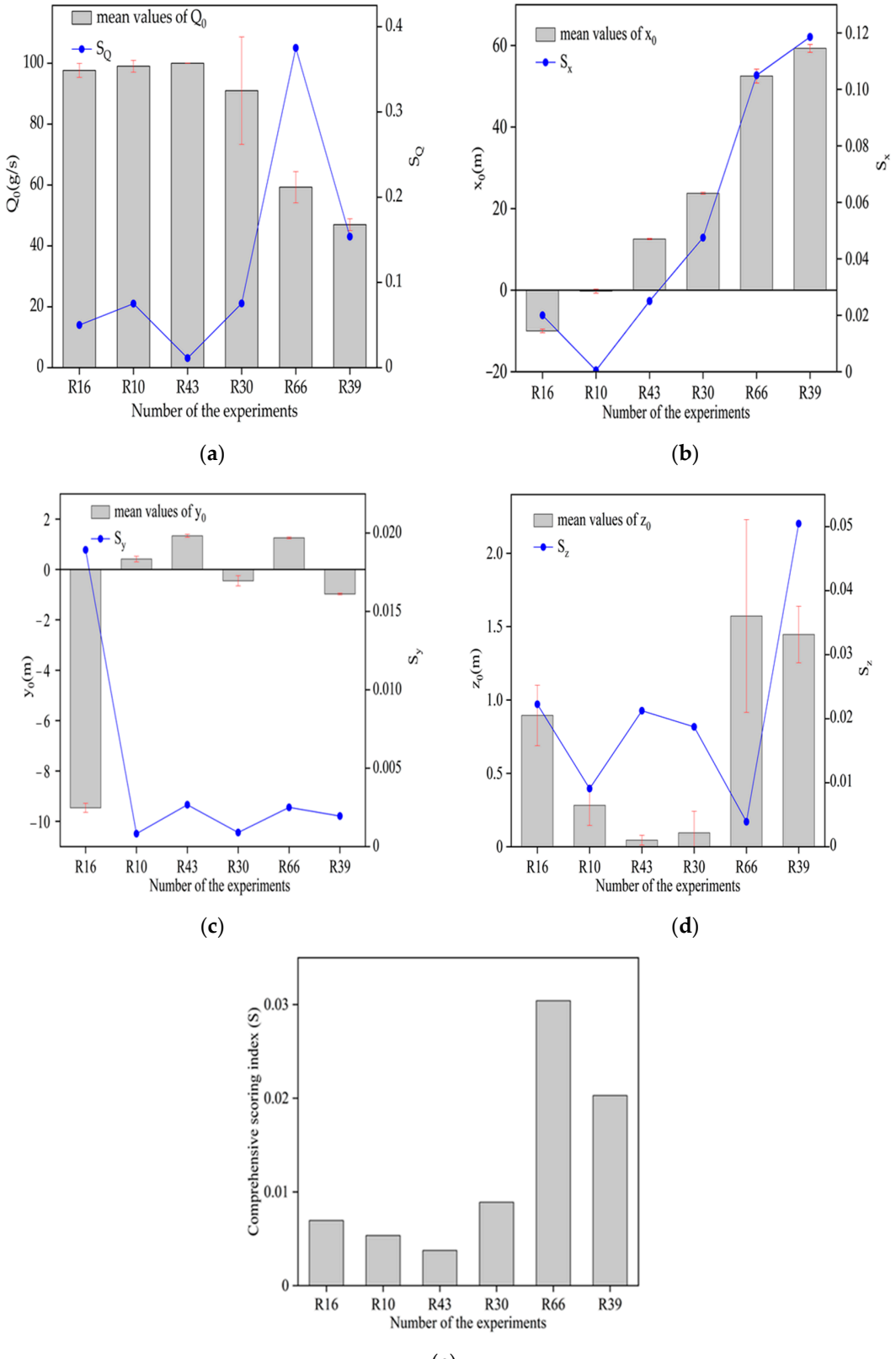

Figure 4. Estimated results of the source parameters of trials under various stability classes based on 10 independent runs of the PSO, denoted by mean values (gray bars) and 95% confidence intervals (red error bars): (**a**) estimation results of source strength (Q_0); (**b**) estimation results of location (x_0); (**c**) estimation results of location (y_0); (**d**) estimation results of location (z_0); (**e**) comprehensive scoring index (S).

It is noteworthy that estimated outcomes for source strength Q_0 and horizontal locations x_0, y_0 were worse under extreme (strongly unstable and more stable) diffusion conditions, such as the estimated outcomes of R16, R66, and R39 (conducted under strongly unstable, more stable, and stable diffusion conditions, respectively), and were not as good as estimated outcomes of tests conducted under other diffusion conditions. It is likely that the limitations of the Gaussian model and the poor quality of the observed concentration data result in parameter estimation results that deviate significantly from the actual values.

Figure 5 shows observed and simulated concentration distributions for the six trials selected, with the exception of R66 and R16, where there were some variations between the simulated and observed gas dispersion directions. For the remaining tests, the simulated and observed concentration distributions, leak source locations, and gas dispersion directions are accurately reconstructed, as shown in Figure 5.

Figure 3 compares observed and simulated concentration values by the Gaussian model for the six trials selected. In Figure 3a,e, there is a certain deviation between observation and simulation concentrations by Gaussian models for R16 and R66, which have a lower correlation coefficient COR between the observation and simulation concentrations of 0.81 and 0.78, respectively, compared to the remaining tests. There was an offset in the location of the peak concentration of R16 and the crosswind profiles of the actual observed concentrations for R16 and R66 showed bimodal distributions, whereas the crosswind profiles of the simulated concentrations by the Gaussian model for R16 and R66 showed unimodal distributions, where the bimodal distributions may have occurred due to changes in the wind direction during the experiment. This indicates that certain limitations exist in the Gaussian diffusion model itself, which does not account for the impact of meteorological conditions on the simulations.

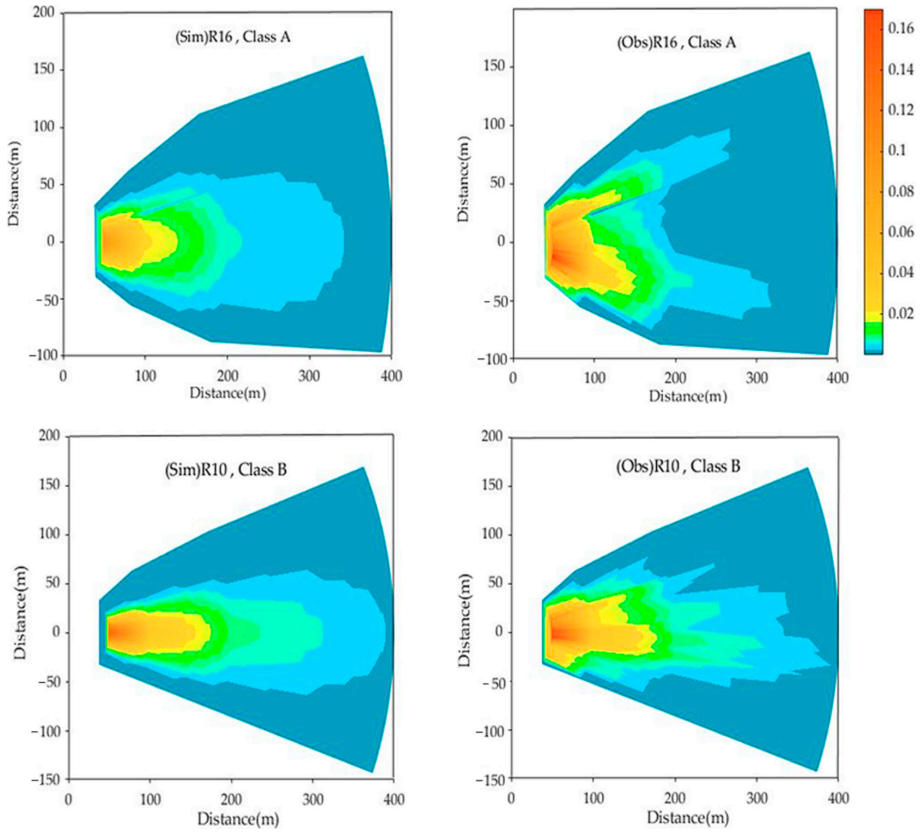

Figure 5. *Cont*.

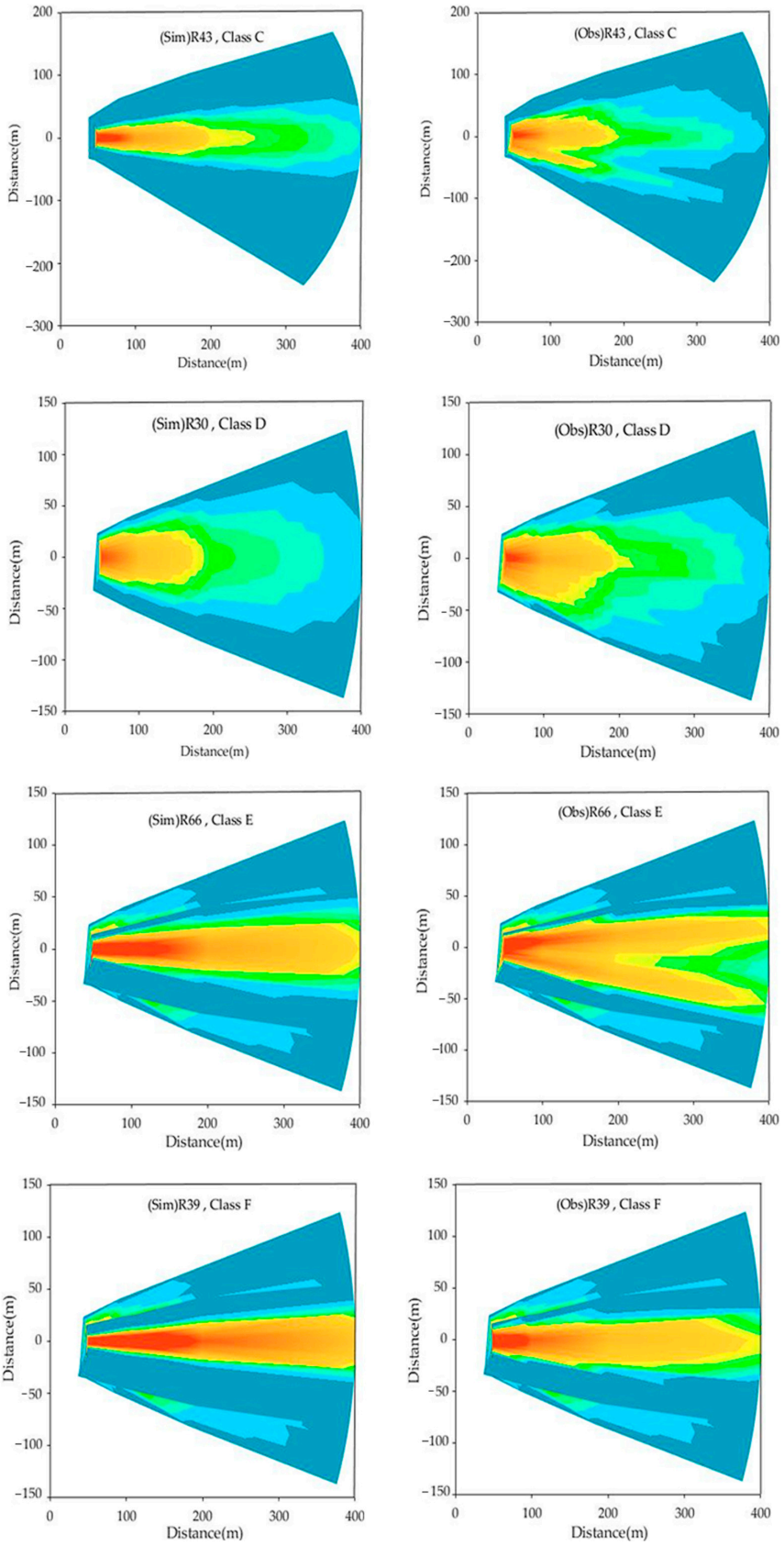

Figure 5. Concentration distribution of the prairie grass experiment under stability classes A to F. (**Left**) concentration distribution simulated by the Gaussian model utilizing experimental parameters; (**Right**) concentration distribution of actual observations of the prairie grass experiment.

3.2. Improvement of Gaussian Dispersion Model in Source-Term Estimation

As discussed in Section 2.1, the precision of the forward diffusion model had an effect on the estimated outcomes of source parameters. The experimental data of the prairie grass experiment were found to approach the Gaussian distribution; observed concentrations from the experiments agreed well with the simulated results from the Gaussian dispersion models. Consequently, the Gaussian dispersion model, which is simple and efficient, was adopted for the estimation of the source-term parameters. Nevertheless, the concentrations simulated by the Gaussian dispersion model were unlikely to adequately represent the concentrations from the actual diffusion of the gas under extreme atmospheric diffusion conditions, and there were inconsistencies and deviations between the concentrations simulated by the Gaussian dispersion model and concentrations observed from the experiment, as illustrated in the discussion of the estimated effects of the source terms for R16 and R66 and presented in Figures 3 and 5. By adding correction coefficients to the Gaussian dispersion model to enhance the precision of the estimated outcomes of source parameters due to the inapplicability of the Gaussian diffusion model under extreme atmospheric diffusion conditions, the objective function evolves into (10), (11) from Equation (2):

$$f(Q_0, x_0, y_0, z_0) = \min \sum_{i=1}^{n} [C_{mon,i} - (c_1 \cdot C_{cal,i}(Q, x, y, z) + c_2)]^2 \quad (10)$$

$$f(Q_0, x_0, y_0, z_0) = \min \sum_{i=1}^{n} \left[C_{mon,i} - \left(a \cdot C_{cal,i}(Q, x, y, z)^2 + b \cdot C_{cal,i}(Q, x, y, z) + c \right) \right]^2 \quad (11)$$

where [c_1, c_2] are linear correction coefficients and [a, b, c] are polynomial correction coefficients, which are obtained from the correlation analysis between the experimental data and Gaussian diffusion model simulation results. The 68 trials were divided by atmospheric stability classes A to F. According to the releases of the experiment under stability classes A to F, the simulated results of the Gaussian dispersion model were fitted with the experiment data by linear least square and polynomial, respectively, which obtained the linear correction coefficients [c_1, c_2] and polynomial correction coefficients [a, b, c] under the stability classes A~F. The fitting results under various atmospheric stability classes are illustrated in Figure 6.

The linear and polynomial correction coefficients under various stability classes were integrated into the Gaussian dispersion model to enhance the estimated outcomes of the source parameters. Figure 7 shows the prediction performance of the Gaussian dispersion model, the Gaussian dispersion model with the linear correction coefficients and Gaussian model with the polynomial correction coefficients on the experimental cases R16 and R66. The prediction results for various diffusion models are presented in Table 2. The results demonstrate that integrating the correction coefficients into the Gaussian dispersion model can enhance its prediction precision. The prediction results of the Gaussian dispersion model with correction coefficients have lower root mean square errors (RMSEs) and higher correlation coefficients (CORs).

Table 2. Comparison the prediction results of different diffusion models of R16 and R66.

Model	R16		R66	
	RMSE	**COR**	**RMSE**	**COR**
Gaussian model	0.026941	0.81442	0.079089	0.77518
Linear modified Gaussian model	0.026391	0.81442	0.051129	0.77552
Polynomial modified Gaussian model	0.025901	0.82765	0.049533	0.80841

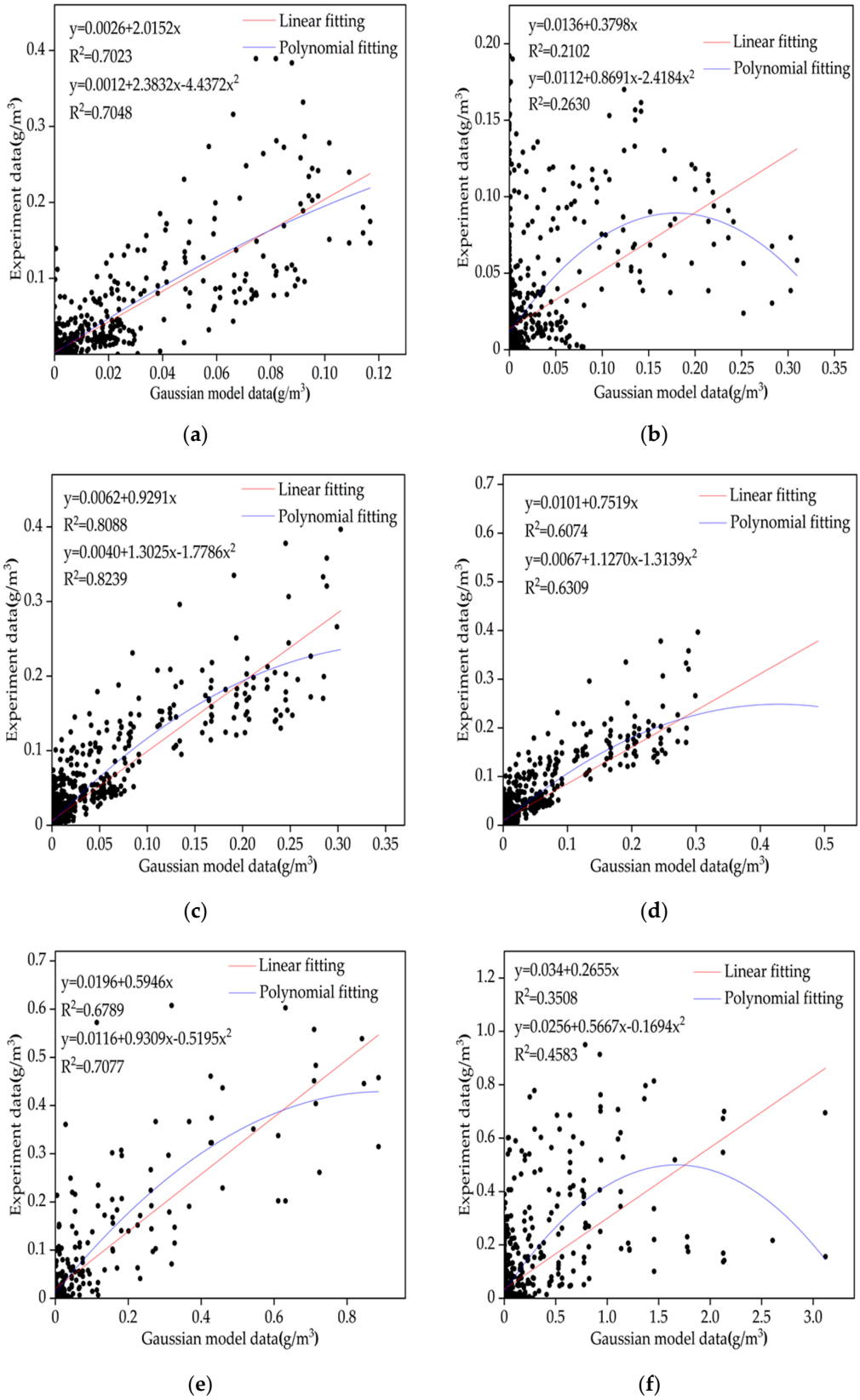

Figure 6. Comparison of experimental data and simulated results of Gaussian models under stability classes A to F: (**a**) fitting for data under stability class A; (**b**) fitting for data under stability class B; (**c**) fitting for data under stability class C; (**d**) fitting for data under stability class D; (**e**) fitting for data under stability class E; (**f**) fitting for data under stability class F.

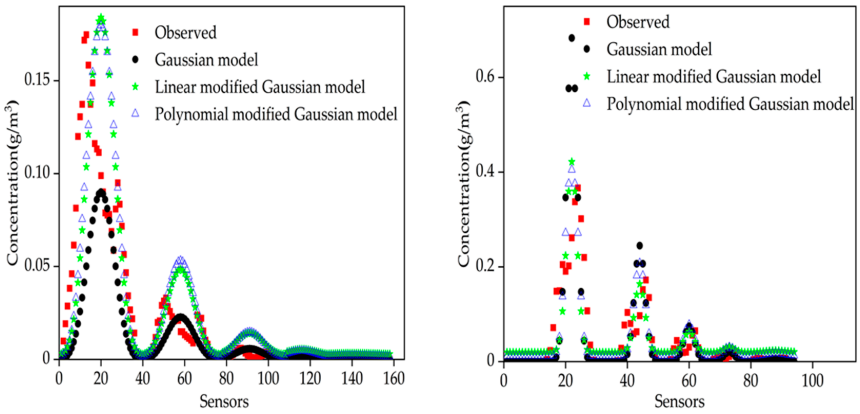

Figure 7. Comparison of observation and simulation concentrations of models (Gaussian, linear modified Gaussian, and polynomial modified Gaussian models) for R16 and R66: (**a**) R16; (**b**) R66.

Hence, the values of the linear [c_1, c_2] and polynomial [a, b, c] correction coefficients under stability classes A and E were employed to identify the source parameters for R16 and R66, respectively. Figure 8 compares the score indexes of source parameters of various objective functions with and without correction coefficients utilizing the experiment data of experimental cases R16 and R66. The results demonstrate that the score indexes of the source parameters of the objective function with correction coefficients are less than those of the objective function without correction coefficients, which implies that the addition of correction coefficients enhances the precision of the estimated outcomes of source parameters. Additionally, it was discovered that the performances of the source-term estimations of the model with linear correction coefficients and model with polynomial correction coefficients were significantly different under different diffusion conditions. For experimental case R16 (stability class A), the estimated performance of the source terms of the model with polynomial correction coefficients outperformed model with linear correction coefficients; however, the reverse was true for experimental case R66 (stability class E).

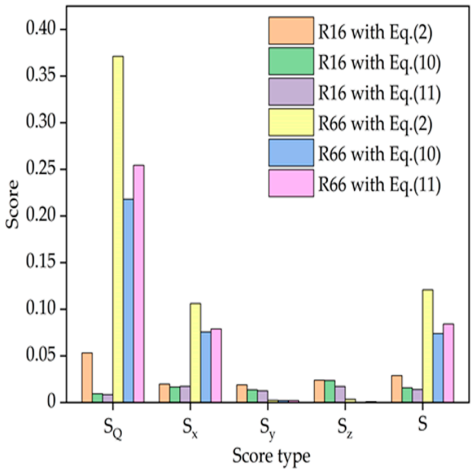

Figure 8. Different score indexes of R16 and R66 with Equations (2), (10) and (11).

Therefore, studying the estimated performance of the source-term parameters of the two modified models under various atmospheric diffusion conditions can provide a reference for model selection in practical applications. Based on all 68 experimental cases, the values of the linear [c_1, c_2] and polynomial [a, b, c] correction coefficients under various atmospheric stability classes were employed to identify the source parameters of the tests under the corresponding atmospheric stability classes. Figure 9 compares the score indexes of various objective functions with linear and polynomial correction

coefficients and without correction coefficients for source-term parameters under stability classes A to F.

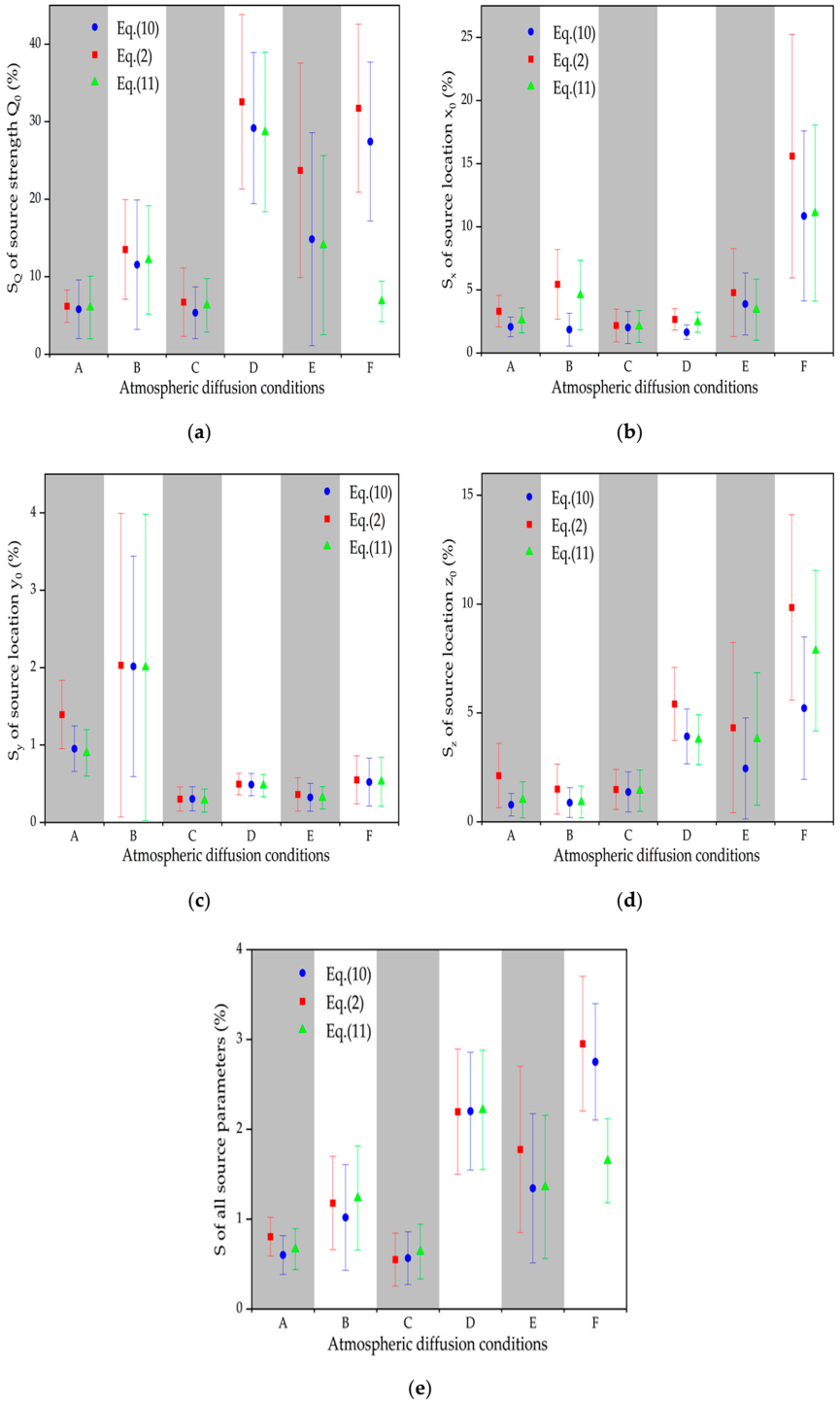

Figure 9. Score indexes of different objective functions for source-term parameters under stability classes A to F: (**a**) score index S_Q of source strength Q_0 of different objective functions under stability classes A to F; (**b**) score index S_x of horizontal location x_0 of different objective functions under stability classes A to F; (**c**) score index S_y of horizontal location y_0 of different objective functions under stability classes A to F; (**d**) score index S_z of location parameter z_0 of different objective functions under stability classes A to F; (**e**) comprehensive score index S of all source parameters [Q_0, x_0, y_0, z_0] of different objective functions under stability classes A to F.

The following conclusions can be drawn from Figure 9:

(1) For all source parameters [Q_0, x_0, y_0, z_0], comparing the estimation results of different models, the Gaussian model with linear coefficients performed the best with the lowest comprehensive score index S under stability classes A (0.6%), B (1.0%), and C (0.5%), respectively (Figure 9e), whereas the Gaussian model with polynomial coefficients performed the best with the lowest comprehensive score index S under stability classes E (1.3%) and F (1.6%), respectively. This indicated that the performance of the Gaussian model with linear correction coefficients for estimating all source parameters [Q_0, x_0, y_0, z_0] outperformed the Gaussian model with polynomial correction coefficients under stability classes A to C. The opposite was true under stability classes E and F; the performance of the two correction models did not vary obviously under stability class D.

(2) For source strength Q_0, the estimation performance of all models showed significant fluctuations under all diffusion conditions (Figure 9a). The worst performance appeared in stability classes D, E, and F. Comparing the estimation results of different models, the Gaussian model had the worst performance with the highest score index S_Q under stability classes A (6.1%), B (13.4%), C (6.6%), D (32.4%), E (23.6%), and F (31.6%), respectively. While the Gaussian model with linear coefficients presented the best performance with the lowest score index S_Q under stability classes A (5.8%), B (11.5%), and C (5.4%), respectively, the Gaussian model with polynomial coefficients performed the best with the lowest score index S_Q under stability classes D (28.6%), E (14.0%), and F (6.8%), respectively. This indicated that the performance of the Gaussian model with linear correction coefficients for estimating source strength Q_0 outperformed the Gaussian model with polynomial correction coefficients under stability classes A to C. However, the opposite was true for stability classes D to F.

(3) For the horizontal location x_0, the estimation performance of all models displayed significant fluctuations under all diffusion conditions (Figure 9b). The worst performance appeared in stability class F. Comparing the estimation results of different models, the Gaussian model had the worst performance with the highest score index S_x under stability classes A (3.3%), B (5.4%), C (2.1%), D (2.6%), E (4.8%), and F (15.6%), respectively. Where the Gaussian model with linear coefficients had the best performance with the lowest score index S_x under stability classes A (2.1%), B (1.9%), and C (2.0%), D (1.7%), and F (10.9%), respectively, the Gaussian model with polynomial coefficients performed the best with the lowest score index S_x under stability class E (3.4%). This indicated that the performance of the Gaussian model with polynomial correction coefficients for estimating horizontal location x_0 outperformed the Gaussian model with linear correction coefficients under stability class E. The opposite was true for the other stability classes.

(4) For horizontal location y_0, the estimation performances of all models were comparable to the similar score index S_y ($0.3 \pm 1.7\%$) under all diffusion conditions (Figure 9c). Overall, the Gaussian model with polynomial coefficients was relatively better than the other two models, with the lowest score index S_y under stability classes A (0.9%), C (0.3%), and D (0.5%), respectively. This indicated that the performance of the Gaussian model with linear correction coefficients for estimating the horizontal location y_0 outperformed the Gaussian model with polynomial correction coefficients under stability classes A, C, and D. However, the performance of the two correction models did not vary obviously under other stability classes.

(5) For location parameter z_0, comparing the estimation results of different models, the Gaussian model had the worst performance with the highest score index S_z under stability classes A (2.0%), B (1.5%), C (1.4%), D (5.4%), E (4.3%), and F (9.8%), respectively (Figure 9d). Where the Gaussian model with linear coefficients had the best performance with the lowest score index S_z under stability classes A (0.7%), C (1.3%), E (2.4%), and F (5.2%), respectively, the Gaussian model with polynomial coefficients performed the best with the lowest score index S_z under stability class

D (3.7%). This indicated that the performance of the Gaussian model with linear correction coefficients for estimating location parameter z_0 outperformed the model with polynomial correction coefficients under stability classes A, C, E, and F. The opposite was true for stability class D; the performance of the two correction models did not vary obviously under stability class B.

As discussed above, applying the two proposed correction models can increase the estimated precision of source parameters under all diffusion conditions. However, the estimated precision of the two correction models varied for different source-term parameters under various diffusion conditions, and there was no single optimal model. Hence, if enhancing the estimated precision of a certain source-term parameter or the overall source-term parameters was desired, the model could be selected according to the practical diffusion conditions, and the specific model selection scheme is provided in Table 3. The conclusions attained in this paper may offer some reference for selecting models in practical diffusion conditions. However, this paper conducted the research utilizing the experimental cases from the prairie grass field dispersion experiment, which was conducted on a flat terrain with almost no obstacles, and the Gaussian model was able to simulate gas dispersion relatively well in this ideal terrain. It could restrict the application of the proposed modified model in a complex terrain. Thus, appropriate dispersion model schemes for complex terrains need to be assessed further.

Table 3. Model selection scheme in practical applications.

Atmospheric Diffusion Conditions	A	B	C	D	E	F
Q_0	(10)	(10)	(10)	(11)	(11)	(11)
x_0	(10)	(10)	(10)	(10)	(11)	(10)
y_0	(11)	(10)/(11)	(11)	(11)	(10)/(11)	(10)/(11)
z_0	(10)	(10)/(11)	(10)	(11)	(10)	(10)
$[Q_0, x_0, y_0, z_0]$	(10)	(10)	(10)	(10)/(11)	(11)	(11)

4. Conclusions

This work verified the effectiveness of PSO algorithms based on the Gaussian plume dispersion model for identifying leakage source parameters and analyzed its performance for source-term estimations. Cases from the prairie grass field experiment were used to test the algorithm. The model was also optimized to enhance the estimated precision of source-term parameters due to the inapplicability of the Gaussian dispersion model under extreme diffusion conditions.

The proposed source-term estimation method was examined and the effect of atmospheric diffusion conditions on estimation outcomes was emphasized, utilizing experimental cases under various diffusion conditions. The findings indicate that estimated results of source-term parameters under extreme diffusion conditions are not as good as under other diffusion conditions, with some deviations between the estimates and actual values of the source-term parameters; however, the estimated precision of source-term parameters was within an acceptable scope.

It was also discovered that the lower the deviation of the simulated concentration by the Gaussian dispersion model from the actual observed concentration, the better the estimated performance of the source-term parameters. Consequently, the Gaussian dispersion model was optimized by introducing correction coefficients into it for the purpose of enhancing the estimated precision of source-term parameters. By fitting the data of 68 experimental cases with the simulation results of the Gaussian model by linear and polynomial methods, respectively, we obtained linear and polynomial correction coefficients under different stability classes. The test results show that the improved Gaussian dispersion model is employed as a forward diffusion model in the PSO algorithm, which enhances the estimated precision of the PSO algorithm.

Furthermore, the performance of Gaussian dispersion models with linear correction coefficients and Gaussian dispersion models with polynomial correction coefficients for estimating the source-term parameters under various atmospheric stability classes was discussed. The results show that the performances of two correction models differ significantly under various atmospheric stability classes. There was no single optimal model; however, the model could be selected according to the practical diffusion conditions to enhance the estimated effect of a certain parameter or the overall source-term parameters. The conclusions determined in this paper can provide a reference for model selections in practical diffusion conditions.

Author Contributions: Conceptualization, software, validation, visualization, investigation, methodology, formal analysis, and writing—original draft preparation, J.L. and M.H.; supervision, funding acquisition, and writing—review and editing, W.W.; resources and data curation, Y.W.; resources, C.L. All authors have read and agreed to the published version of the manuscript.

Funding: This work was supported by the Zhoushan Science and Technology Bureau under (grant number 2022C41007).

Institutional Review Board Statement: Not applicable.

Informed Consent Statement: Not applicable.

Data Availability Statement: Not applicable.

Conflicts of Interest: The authors declare no conflict of interest.

References

1. Hutchinson, M.; Oh, H.; Chen, W.H. A review of source term estimation methods for atmospheric dispersion events using static or mobile sensors. *Inf. Fusion* **2016**, *36*, 130–148. [CrossRef]
2. Albani, R.A.S.; Albani, V.V.L.; Neto, A.J.S. Source Characterization of Airborne Pollutant Emissions by Hybrid Metaheuristic/Gradient-based Optimization Techniques. *Environ. Pollut.* **2020**, *267*, 115618. [CrossRef] [PubMed]
3. Mao, S.S.; Lang, J.L.; Chen, T.; Cheng, S.Y. Improving source inversion performance of airborne pollutant emissions by modifying atmospheric dispersion scheme through sensitivity analysis combined with optimization model. *Environ. Pollut.* **2021**, *284*, 117186. [CrossRef] [PubMed]
4. Cui, J.X.; Lang, J.L.; Chen, T.; Cheng, S.Y.; Shen, Z.Y.; Mao, S.S. Investigating the impacts of atmospheric diffusion conditions on source parameter identification based on an optimized inverse modelling method. *Atmos. Environ.* **2019**, *205*, 19–29. [CrossRef]
5. Mao, S.S.; Hu, F.; Lang, J.L.; Chen, T.; Cheng, S.Y. Comparative Study of Impacts of Typical Bio-Inspired Optimization Algorithms on Source Inversion Performance. *Front. Environ. Sci.* **2022**, *10*, 894255. [CrossRef]
6. Guohua, C.; Longkai, C. Enhancing Situation Awareness of Chemical Release Through Source Inversion. *Procedia Eng.* **2014**, *84*, 742–751. [CrossRef]
7. Wang, Y.; Huang, H.; Huang, L.D.; Ristic, S. Evaluation of Bayesian source estimation methods with Prairie Grass observations and Gaussian plume model: A comparison of likelihood functions and distance measures. *Atmos. Environ.* **2017**, *152*, 519–530. [CrossRef]
8. Keats, A.; Yee, E.; Lien, F.S. Bayesian inference for source determination with applications to a complex urban environment. *Atmos. Environ.* **2007**, *41*, 465–479. [CrossRef]
9. Senocak, I.; Hengartner, N.W.; Short, M.B.; Daniel, W.B. Stochastic Event Reconstruction of Atmospheric Contaminant Dispersion using Bayesian Inference. *Atmos. Environ.* **2008**, *42*, 7718. [CrossRef]
10. Ristic, B.; Gunatilaka, A.; Gailis, R.; Skvortsov, A. Bayesian likelihood-free localisation of a biochemical source using multiple dispersion models. *Signal Process.* **2015**, *108*, 13–24. [CrossRef]
11. Ma, D.; Deng, J.; Zhang, Z. Comparison and improvements of optimization methods for gas emission source identification. *Atmos. Environ.* **2013**, *81*, 188–198. [CrossRef]
12. Wang, Y.; Huang, H.; Huang, L.D.; Zhang, X.L. Source term estimation of hazardous material releases using hybrid genetic algorithm with composite cost functions. *Eng. Appl. Artif. Intell.* **2018**, *75*, 102–113. [CrossRef]
13. Haupt, S.E.; Young, G.S.; Allen, C.T. A Genetic Algorithm Method to Assimilate Sensor Data for a Toxic Contaminant Release. *JCP* **2007**, *2*, 85–93. [CrossRef]
14. Thomson, L.C.; Hirst, B.; Gibson, G.; Gillespie, S.; Jonathan, P.; Skeldon, K.D.; Padgett, M.J. An improved algorithm for locating a gas source using inverse methods. *Atmos. Environ.* **2007**, *41*, 1128–1134. [CrossRef]
15. Cervone, G.; Franzese, P. Non-Darwinian evolution for the source detection of atmospheric releases. *Atmos. Environ.* **2011**, *45*, 4497–4506. [CrossRef]

16. Haupt, S.E.; Young, G.S.; Allen, C.T. Validation of a Receptor–Dispersion Model Coupled with a Genetic Algorithm Using Synthetic Data. *J. Appl. Meteorol. Climatol.* **2006**, *45*, 476–490. [CrossRef]
17. Kennedy, J.; Eberhart, R. Particle Swarm Optimization. In Proceedings of the 1995 IEEE International Conference on Neural Networks, Perth, Australia, 27 November–1 December 1995; pp. 1942–1948.
18. Ma, D.L.; Tan, W.; Wang, Q.S.; Zhang, Z.X.; Gao, J.M.; Zeng, Q.F.; Wang, X.Q.; Xia, F.S.; Shi, X.M. Application and improvement of swarm intelligence optimization algorithm in gas emission source identification in atmosphere. *J. Loss Prev. Process Ind.* **2018**, *56*, 262–271. [CrossRef]
19. Ma, D.L.; Tan, W.; Zhang, Z.X.; Hu, J. Parameter identification for continuous point emission source based on Tikhonov regularization method coupled with particle swarm optimization algorithm. *J. Hazard. Mater.* **2017**, *325*, 239–250. [CrossRef]
20. Qiu, S.; Chen, B.; Wang, R.; Zhu, Z.; Wang, Y.; Qiu, X. Atmospheric dispersion prediction and source estimation of hazardous gas using artificial neural network, particle swarm optimization and expectation maximization. *Atmos. Environ.* **2018**, *178*, 158–163. [CrossRef]
21. Wang, R.; Chen, B.; Qiu, S.; Zhu, Z.; Wang, Y.; Wang, Y.; Qiu, X. Comparison of Machine Learning Models for Hazardous Gas Dispersion Prediction in Field Cases. *Int. J. Environ. Res. Public Health* **2018**, *15*, 1450. [CrossRef]
22. Mao, S.; Lang, J.; Chen, T.; Cheng, S.; Cui, J.; Shen, Z.; Hu, F. Comparison of the impacts of empirical power-law dispersion schemes on simulations of pollutant dispersion during different atmospheric conditions. *Atmos. Environ.* **2020**, *224*, 117317. [CrossRef]
23. Barad, M.L. *Project Prairie Grass: A Field Program in Diffusion*; Geophysical Research Paper; Technical Report AFCRC-TR-58-235(I); Air Force Cambridge Research Center; Wright-Patterson Air Force Base: Hanscom, MA, USA, 1958.
24. Briggs, G.A. *Diffusion Estimation for Small Emissions*; ATDL Contribution File NO.79; National Oceanic and Atmospheric Administration: Oak Ridge, TN, USA, 1973.
25. Zhu, J.J.; Zhou, X.Y.; Cong, B.H.; Kikumoto, H. Estimation of the point source parameters by the adjoint equation in the time-varying atmospheric environment with unknown turn-on time. *Build. Environ.* **2023**, *230*, 110029. [CrossRef]
26. Flesch, T.K.; Wilson, J.D.; Harper, L.A.; Crenna, B.P.; Sharpe, R.R. Deducing Ground-to-Air Emissions from Observed Trace Gas Concentrations: A Field Trial. *J. Appl. Meteorol. Climatol.* **2004**, *43*, 487–502. [CrossRef]
27. Pasquill, F.; Smith, F.B. *Atmospheric Diffusion*, 3rd ed.; Ellis Horwood Limited: Chichester, UK, 1983.

Disclaimer/Publisher's Note: The statements, opinions and data contained in all publications are solely those of the individual author(s) and contributor(s) and not of MDPI and/or the editor(s). MDPI and/or the editor(s) disclaim responsibility for any injury to people or property resulting from any ideas, methods, instructions or products referred to in the content.